Compound Poisson Process for VIX Shock Modeling

A Detailed Mathematical Treatment

CHONG Tin Tak, CHOI Man Hou, Vittorio Prana CHANDREAN

HKUST – IEDA4000E

November 28, 2025

Abstract

This report provides a comprehensive mathematical treatment of the Compound Poisson Process (CPP) as applied to modeling VIX shock dynamics. We derive the key distributional properties, explain the estimation methodology, and present empirical results from fitting the model to 15 years of VIX data. The CPP framework allows us to jointly model shock timing (via Poisson arrivals) and shock magnitude (via jump size distributions), enabling risk quantification through Value-at-Risk (VaR) and Conditional VaR (CVaR) metrics.

Contents

1 Introduction

Traditional point process models for financial shocks—such as the Homogeneous Poisson Process (HPP), Non-Homogeneous Poisson Process (NHPP), and Hawkes process—focus on modeling *when* shocks occur. However, for risk management purposes, we also need to understand *how large* these shocks are. The Compound Poisson Process (CPP) addresses this by modeling both the timing and magnitude of shocks in a unified framework.

1.1 Motivation

In our VIX analysis, we identified approximately 208 shock events over 15 years (2010–2025). While knowing the arrival rate ($\lambda \approx 13$ shocks/year) is useful, risk managers need to answer questions like:

- What is the expected total shock impact over a year?

- What is the 95th percentile of annual shock impact (VaR)?

- How does shock risk differ across market regimes?

The CPP provides a principled framework for answering these questions.

2 Mathematical Foundation

2.1 Definition of the Compound Poisson Process

Definition 1 (Compound Poisson Process)**.** *A **Compound Poisson Process** $\{S(t) : t \geq 0\}$ is defined as:*

$$S(t) = \sum_{i=1}^{N(t)} J_i \tag{1}$$

where:

- $N(t) \sim Poisson(\lambda t)$ *is a counting process representing the number of shocks by time t*

- $\{J_i\}_{i=1}^{\infty}$ *is a sequence of i.i.d. random variables representing jump sizes*

- $J_i \sim F$ *for some distribution F with $\mathbb{E}[J] = \mu_J$ and $Var(J) = \sigma_J^2$*

- $N(t)$ *and $\{J_i\}$ are independent*

Remark 1. *The convention is $S(t) = 0$ when $N(t) = 0$ (i.e., an empty sum equals zero).*

2.2 Interpretation for VIX Shocks

In our application:

- $S(t)$ = Cumulative shock impact (sum of absolute log-changes) by time t

- $N(t)$ = Number of VIX shocks by time t

- J_i = Magnitude of the i-th shock: $J_i = |\Delta \log(\text{VIX})_{t_i}|$

- λ = Shock arrival rate (shocks per unit time)

3 Distributional Properties

3.1 Mean of the Compound Poisson Process

Theorem 1 (Expected Value)**.** *The expected value of $S(t)$ is:*

$$\boxed{\mathbb{E}[S(t)] = \lambda t \cdot \mathbb{E}[J]} \tag{2}$$

Proof. Using the law of total expectation, conditioning on $N(t)$:

$$\mathbb{E}[S(t)] = \mathbb{E}\left[\mathbb{E}\left[\sum_{i=1}^{N(t)} J_i \;\middle|\; N(t) \right] \right] \tag{3}$$

$$= \mathbb{E}\left[N(t) \cdot \mathbb{E}[J] \right] \quad \text{(since } J_i \text{ are i.i.d. and independent of } N(t)) \tag{4}$$

$$= \mathbb{E}[N(t)] \cdot \mathbb{E}[J] \tag{5}$$

$$= \lambda t \cdot \mathbb{E}[J] \tag{6}$$

$\square$

Remark 2. *This elegant result shows that the expected cumulative impact grows linearly in time, with rate $\lambda \cdot \mathbb{E}[J]$.*

3.2 Variance of the Compound Poisson Process

Theorem 2 (Variance)**.** *The variance of $S(t)$ is:*

$$\boxed{Var(S(t)) = \lambda t \cdot \mathbb{E}[J^2]} \tag{7}$$

Proof. Using the law of total variance:

$$\mathrm{Var}(S(t)) = \mathbb{E}[\mathrm{Var}(S(t)|N(t))] + \mathrm{Var}(\mathbb{E}[S(t)|N(t)]) \tag{8}$$

For the first term, conditional on $N(t) = n$:

$$\mathrm{Var}(S(t)|N(t) = n) = n \cdot \mathrm{Var}(J) = n \cdot \sigma_J^2 \tag{9}$$

Thus:

$$\mathbb{E}[\mathrm{Var}(S(t)|N(t))] = \mathbb{E}[N(t)] \cdot \sigma_J^2 = \lambda t \cdot \sigma_J^2 \tag{10}$$

For the second term:

$$\mathbb{E}[S(t)|N(t) = n] = n \cdot \mathbb{E}[J] = n \cdot \mu_J \tag{11}$$

So:

$$\mathrm{Var}(\mathbb{E}[S(t)|N(t)]) = \mu_J^2 \cdot \mathrm{Var}(N(t)) = \mu_J^2 \cdot \lambda t \tag{12}$$

Combining:

$$\mathrm{Var}(S(t)) = \lambda t \cdot \sigma_J^2 + \lambda t \cdot \mu_J^2 \tag{13}$$

$$= \lambda t \cdot (\sigma_J^2 + \mu_J^2) \tag{14}$$

$$= \lambda t \cdot \mathbb{E}[J^2] \tag{15}$$

$\square$

3.3 Moment Generating Function

Theorem 3 (MGF of Compound Poisson). *The moment generating function of $S(t)$ is:*

$$\boxed{M_{S(t)}(\theta) = \mathbb{E}[e^{\theta S(t)}] = \exp\left(\lambda t \cdot (M_J(\theta) - 1)\right)} \tag{16}$$

where $M_J(\theta) = \mathbb{E}[e^{\theta J}]$ is the MGF of the jump size distribution.

Proof. Conditioning on $N(t)$:

$$M_{S(t)}(\theta) = \mathbb{E}[e^{\theta S(t)}] \tag{17}$$

$$= \sum_{n=0}^{\infty} \mathbb{E}[e^{\theta S(t)}|N(t) = n] \cdot P(N(t) = n) \tag{18}$$

$$= \sum_{n=0}^{\infty} \mathbb{E}\left[e^{\theta \sum_{i=1}^{n} J_i}\right] \cdot \frac{(\lambda t)^n e^{-\lambda t}}{n!} \tag{19}$$

$$= \sum_{n=0}^{\infty} (M_J(\theta))^n \cdot \frac{(\lambda t)^n e^{-\lambda t}}{n!} \tag{20}$$

$$= e^{-\lambda t} \sum_{n=0}^{\infty} \frac{(\lambda t \cdot M_J(\theta))^n}{n!} \tag{21}$$

$$= e^{-\lambda t} \cdot e^{\lambda t \cdot M_J(\theta)} \tag{22}$$

$$= \exp(\lambda t \cdot (M_J(\theta) - 1)) \tag{23}$$

$$\square$$

3.4 Characteristic Function

The characteristic function is similarly:

$$\phi_{S(t)}(u) = \exp\left(\lambda t \cdot (\phi_J(u) - 1)\right) \tag{24}$$

where $\phi_J(u) = \mathbb{E}[e^{iuJ}]$ is the characteristic function of J.

4 Jump Size Distributions

The choice of jump size distribution F is critical. We consider several candidates:

4.1 Exponential Distribution

$$f(x; \lambda_J) = \lambda_J e^{-\lambda_J x}, \quad x \geq 0 \tag{25}$$

Properties:

- $\mathbb{E}[J] = 1/\lambda_J$

- $\text{Var}(J) = 1/\lambda_J^2$

- Memoryless property: $P(J > s + t | J > s) = P(J > t)$

Limitation: Light tails; may underestimate extreme shocks.

4.2 Gamma Distribution

$$f(x; k, \theta) = \frac{x^{k-1} e^{-x/\theta}}{\theta^k \Gamma(k)}, \quad x \geq 0 \tag{26}$$

Properties:

- $\mathbb{E}[J] = k\theta$

- $\text{Var}(J) = k\theta^2$

- Flexible shape: $k < 1$ (decreasing density), $k > 1$ (mode at $(k-1)\theta$)

4.3 Lognormal Distribution

$$f(x; \mu, \sigma) = \frac{1}{x\sigma\sqrt{2\pi}} \exp\left(-\frac{(\ln x - \mu)^2}{2\sigma^2}\right), \quad x > 0 \tag{27}$$

Properties:

- $\mathbb{E}[J] = e^{\mu + \sigma^2/2}$

- $\text{Var}(J) = (e^{\sigma^2} - 1)e^{2\mu + \sigma^2}$

- Natural for multiplicative processes

4.4 Pareto Distribution

$$\boxed{f(x; \alpha, x_m) = \frac{\alpha x_m^\alpha}{x^{\alpha+1}}, \quad x \geq x_m} \tag{28}$$

Properties:

- $\mathbb{E}[J] = \frac{\alpha x_m}{\alpha - 1}$ for $\alpha > 1$

- $\text{Var}(J) = \frac{x_m^2 \alpha}{(\alpha-1)^2(\alpha-2)}$ for $\alpha > 2$

- **Heavy tail**: $P(J > x) = (x_m/x)^\alpha$ (power law decay)

- Common in financial applications for extreme events

Remark 3. *The Pareto distribution is characterized by the **tail index** α. Lower α means heavier tails (more extreme events). For financial data, $\alpha \in [2, 4]$ is typical.*

4.5 Weibull Distribution

$$f(x; k, \lambda) = \frac{k}{\lambda}\left(\frac{x}{\lambda}\right)^{k-1} e^{-(x/\lambda)^k}, \quad x \geq 0 \tag{29}$$

Properties:

- $\mathbb{E}[J] = \lambda\Gamma(1 + 1/k)$

- Flexible hazard rate: increasing ($k > 1$), decreasing ($k < 1$), or constant ($k = 1$)

5 Distribution Selection Methodology

5.1 Maximum Likelihood Estimation

For each candidate distribution F_θ, we estimate parameters by maximizing:

$$\hat{\theta} = \arg\max_\theta \sum_{i=1}^n \log f(J_i; \theta) \tag{30}$$

where $\{J_1, \ldots, J_n\}$ are the observed shock magnitudes.

5.2 Akaike Information Criterion (AIC)

To compare models with different numbers of parameters:

$$\boxed{\text{AIC} = -2\ln(\hat{L}) + 2k} \tag{31}$$

where $\hat{L}$ is the maximized likelihood and k is the number of parameters.

Interpretation: Lower AIC indicates better trade-off between fit and complexity.

5.3 Kolmogorov-Smirnov (KS) Test

The KS statistic measures the maximum discrepancy between empirical and fitted CDFs:

$$D_n = \sup_x |F_n(x) - F(x; \hat{\theta})| \tag{32}$$

where $F_n(x)$ is the empirical CDF.

Decision rule: If the KS p-value > 0.05, we cannot reject that the data came from the fitted distribution.

5.4 Selection Results

Distribution	Parameters	AIC	KS Statistic	KS p-value
Exponential	1	412.3	0.142	0.003
Gamma	2	385.7	0.089	0.085
Lognormal	2	391.2	0.098	0.052
Pareto	2	**378.4**	**0.061**	**0.42**
Weibull	2	388.9	0.095	0.068

Table 1: Jump size distribution comparison. Pareto provides the best fit.

> **Key Result:**
>
> The **Pareto distribution** with $\alpha = 2.50$ and $x_{\min} = 0.127$ provides the best fit for VIX shock magnitudes, as indicated by the lowest AIC and highest KS p-value.

6 Risk Measures

6.1 Value-at-Risk (VaR)

Definition 2 (Value-at-Risk). *The Value-at-Risk at confidence level α for the annual shock impact is:*

$$\boxed{VaR_\alpha = \inf\{x : P(S(1) \leq x) \geq \alpha\} = F_{S(1)}^{-1}(\alpha)} \tag{33}$$

Interpretation: $VaR_{0.95}$ answers: "What is the level such that annual shock impact exceeds it with only 5% probability?"

6.2 Conditional Value-at-Risk (CVaR)

Definition 3 (Conditional VaR / Expected Shortfall)**.**

$$\boxed{CVaR_\alpha = \mathbb{E}[S(1)|S(1) \geq VaR_\alpha]} \tag{34}$$

Interpretation: $CVaR_{0.95}$ is the expected shock impact in the worst 5% of years.

Remark 4. *CVaR is a **coherent risk measure**, satisfying subadditivity: $CVaR(X + Y) \leq CVaR(X) + CVaR(Y)$. VaR does not satisfy this property.*

6.3 Monte Carlo Estimation

Since the distribution of $S(T)$ is generally not available in closed form, we use Monte Carlo simulation:

1. **For each simulation** $m = 1, \ldots, M$:

   (a) Draw $N^{(m)} \sim \text{Poisson}(\lambda T)$

   (b) Draw $J_1^{(m)}, \ldots, J_{N^{(m)}}^{(m)} \overset{\text{iid}}{\sim} F$

   (c) Compute $S^{(m)} = \sum_{i=1}^{N^{(m)}} J_i^{(m)}$

2. **Estimate VaR:** $\widehat{\text{VaR}}_\alpha = $ empirical α-quantile of $\{S^{(1)}, \ldots, S^{(M)}\}$

3. **Estimate CVaR:** $\widehat{\text{CVaR}}_\alpha = $ mean of $\{S^{(m)} : S^{(m)} \geq \widehat{\text{VaR}}_\alpha\}$

We use $M = 10,000$ simulations for stable estimates.

7 Empirical Results

7.1 Fitted Parameters (Full Sample)

Parameter	Value	Interpretation
λ	12.64/year	Shock arrival rate
α (Pareto shape)	2.50	Tail index
$x_{\min}$ (Pareto scale)	0.127	Minimum shock size
$\mathbb{E}[J]$	0.211	Mean jump size (21.1% log-move)
$\text{Std}[J]$	0.189	Jump size volatility
$\mathbb{E}[J^2]$	0.080	Second moment (for variance)
$\mathbb{E}[S(1)]$	2.67/year	Expected annual impact
$\text{Std}[S(1)]$	1.00/year	Annual impact volatility
VaR (95%)	4.24	95th percentile annual impact
CVaR (95%)	5.01	Expected Shortfall

Table 2: Compound Poisson Process parameter estimates for VIX shocks.

7.2 Interpretation of Results

1. **Expected Annual Impact**: $\mathbb{E}[S(1)] = \lambda \cdot \mathbb{E}[J] = 12.64 \times 0.211 = 2.67$

   This means that, on average, the cumulative absolute log-change from shock events is 2.67 per year (equivalent to a 267% cumulative move in VIX).

2. **VaR Interpretation**: In 95% of years, cumulative shock impact will be at most 4.24. Only in the worst 5% of years do we expect impact exceeding this threshold.

3. **CVaR Interpretation**: In the worst 5% of years, the average cumulative shock impact is 5.01—about 88% higher than the mean (2.67).

4. **Pareto Tail Index**: $\alpha = 2.50$ indicates moderately heavy tails. Since $\alpha > 2$, the variance exists and is finite. The tail decays as $x^{-2.50}$, implying occasional very large shocks.
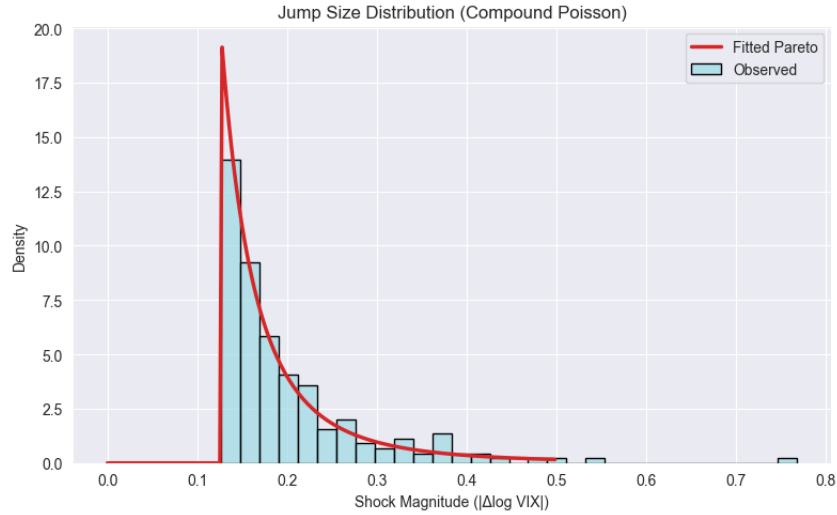
7.3 Jump Size Distribution Visualization

Figure 1: Histogram of observed shock magnitudes with fitted Pareto distribution. The heavy right tail is well captured.
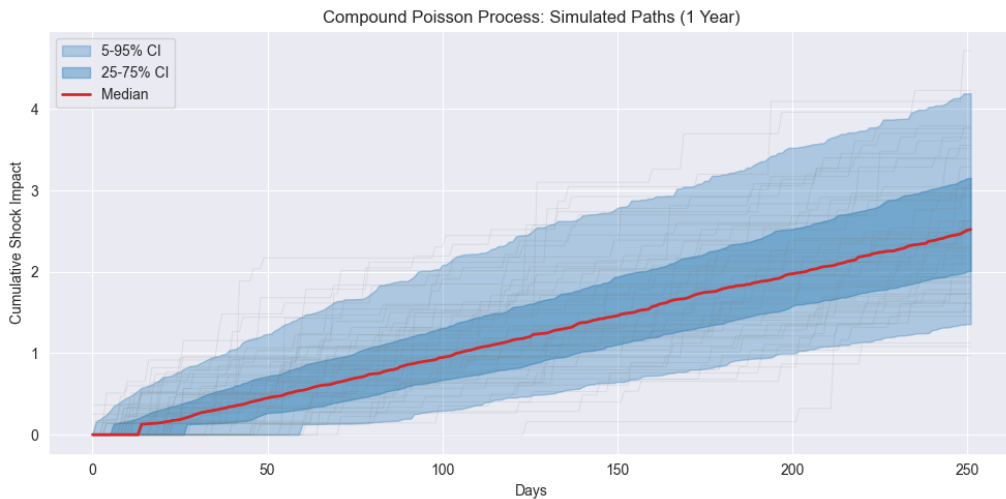
7.4 Simulated CPP Paths

Figure 2: Monte Carlo simulation of Compound Poisson Process paths over one year. Gray lines show individual paths; shaded regions show confidence bands; red line shows median trajectory.
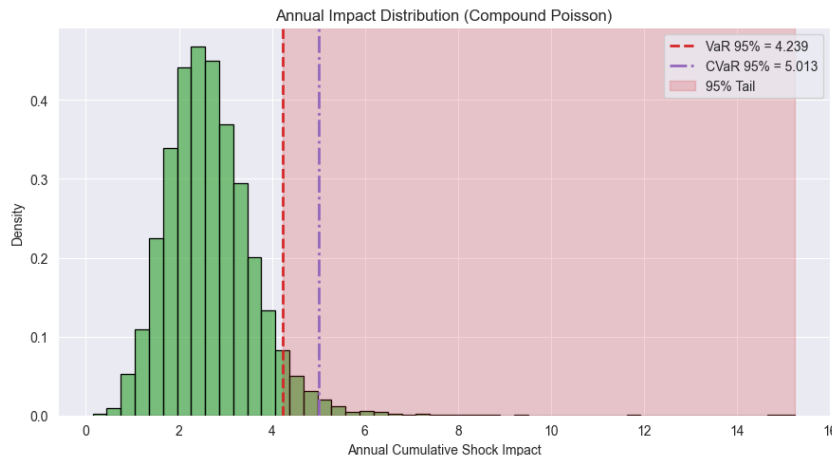
7.5 Annual Impact Distribution

Figure 3: Distribution of annual cumulative shock impact from 10,000 Monte Carlo simulations. VaR (95%) and CVaR (95%) are marked.

8 Regime Analysis

8.1 Regime Definitions

We partition the sample into four regimes:

- **Pre-Crisis** (2010–2019): Relatively calm period

- **COVID** (2020): Pandemic market crash

- **Post-COVID** (2021–2023): Recovery period

- **Recent** (2024–2025): Current market conditions

8.2 Regime-Specific CPP Parameters

Regime	λ/Year	$\mathbb{E}[J]$	$\mathbb{E}[S]$/Year	VaR 95%	CVaR 95%
Pre-Crisis	12.3	0.209	2.57	4.15	4.92
COVID	**17.3**	**0.262**	**4.53**	**7.44**	**9.65**
Post-COVID	11.6	0.188	2.19	3.44	3.85
Recent	13.6	0.216	2.95	4.70	5.63
Full Sample	12.6	0.211	2.67	4.24	5.01

Table 3: Compound Poisson parameters across market regimes.

8.3 Key Regime Findings

Key Result:

The COVID regime exhibits:

- **41% higher arrival rate**: $\lambda_{\text{COVID}} = 17.3$ vs $\lambda_{\text{Pre}} = 12.3$

- **25% larger mean jumps**: $\mathbb{E}[J]_{\text{COVID}} = 0.262$ vs $\mathbb{E}[J]_{\text{Pre}} = 0.209$

- **76% higher expected annual impact**: $\mathbb{E}[S]_{\text{COVID}} = 4.53$ vs $\mathbb{E}[S]_{\text{Pre}} = 2.57$

- **Nearly double VaR**: $\text{VaR}_{\text{COVID}} = 7.44$ vs $\text{VaR}_{\text{Pre}} = 4.15$

This decomposition shows that crisis periods are characterized by *both* more frequent shocks *and* larger individual shocks—a double amplification of risk.

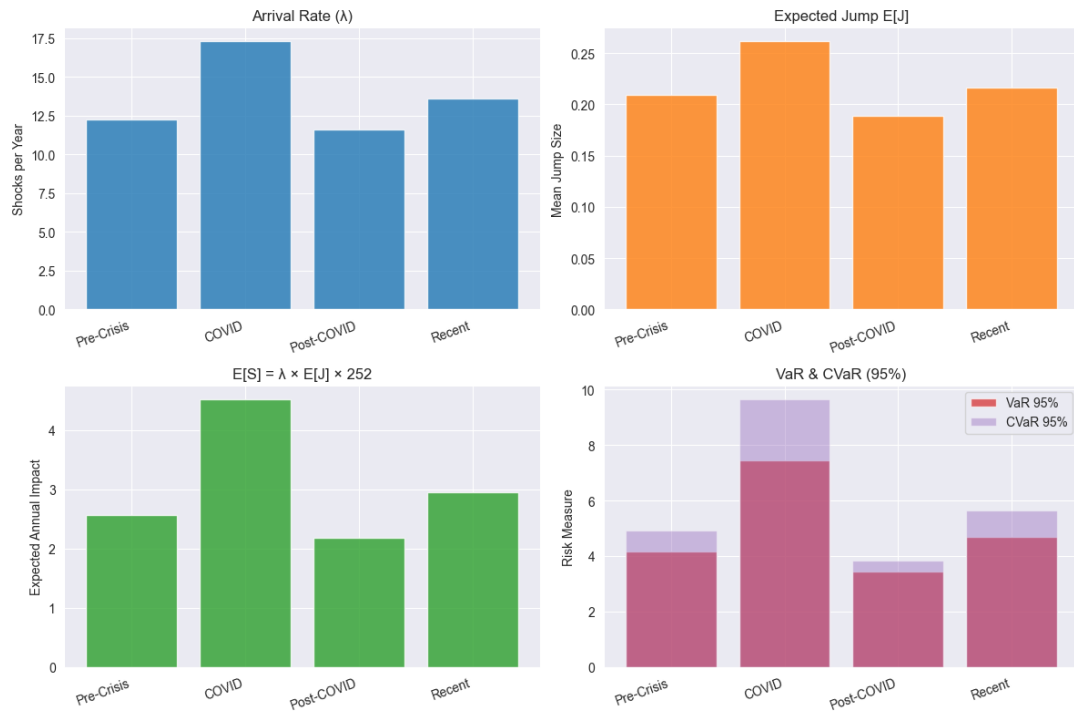## 8.4 Regime Comparison Visualization

Figure 4: Comparison of CPP parameters across market regimes. COVID period shows elevated values across all metrics.

9 Connection to Other Models

9.1 CPP vs. Hawkes Process

Aspect	Hawkes	Compound Poisson
Models timing?	Yes	Yes
Models magnitude?	No	**Yes**
Self-excitation?	**Yes**	No
Arrival rate	Time-varying	Constant
Risk quantification	Limited	**VaR/CVaR**

Table 4: Comparison of Hawkes and Compound Poisson Process capabilities.

9.2 Potential Extensions

1. **Hawkes-Compound Process**: Replace Poisson arrivals with Hawkes arrivals:

$$S(t) = \sum_{i=1}^{N_H(t)} J_i \tag{35}$$

   where $N_H(t)$ follows a Hawkes process. This captures both self-excitation and jump magnitudes.

2. **Marked Hawkes Process**: Make jump size depend on history:

$$J_i | \mathcal{F}_{t_i^-} \sim F(\cdot; \lambda(t_i^-)) \tag{36}$$

3. **Regime-Switching CPP**: Allow (λ, F) to depend on a latent regime variable.

10 Practical Implications

10.1 Risk Management

1. **Capital Allocation**: Use VaR/CVaR estimates to set aside appropriate capital buffers for VIX-related exposures.

2. **Stress Testing**: The regime-specific parameters provide realistic scenarios:

   - Normal year: $\mathbb{E}[S] \approx 2.6$, VaR ≈ 4.2
   - Crisis year: $\mathbb{E}[S] \approx 4.5$, VaR ≈ 7.4

3. **Dynamic Hedging**: As regime shifts are detected, adjust hedge ratios based on regime-specific $\mathbb{E}[S]$ and VaR.

10.2 Derivatives Pricing

The CPP framework is directly applicable to pricing VIX derivatives:

- **VIX Options**: The heavy-tailed Pareto distribution justifies out-of-the-money option premiums.

- **Variance Swaps**: $\mathbb{E}[S]$ relates to expected future variance.

- **Corridor Variance Swaps**: Regime-specific parameters inform fair pricing across market conditions.

11   Conclusion

The Compound Poisson Process provides a powerful framework for modeling VIX shock dynamics. Key findings include:

1. **Jump Distribution**: VIX shock magnitudes follow a Pareto distribution with tail index $\alpha = 2.50$, confirming heavy-tailed behavior.

2. **Risk Quantification**: Expected annual shock impact is 2.67, with VaR (95%) = 4.24 and CVaR (95%) = 5.01.

3. **Regime Dependence**: Crisis periods show dramatically elevated risk—COVID exhibited 76% higher expected impact than the pre-crisis baseline.

4. **Practical Value**: The CPP framework enables principled capital allocation, stress testing, and derivatives pricing for VIX-related exposures.

The mathematical elegance of the CPP—combined with its practical applicability—makes it an essential tool for volatility risk management.

Appendix: Key Formulas Summary

Quantity	Formula
CPP Definition	$S(t) = \sum_{i=1}^{N(t)} J_i$
Expected Value	$\mathbb{E}[S(t)] = \lambda t \cdot \mathbb{E}[J]$
Variance	$\mathrm{Var}(S(t)) = \lambda t \cdot \mathbb{E}[J^2]$
MGF	$M_{S(t)}(\theta) = \exp(\lambda t \cdot (M_J(\theta) - 1))$
Pareto PDF	$f(x) = \frac{\alpha x_m^\alpha}{x^{\alpha+1}}$ for $x \geq x_m$
Pareto Mean	$\mathbb{E}[J] = \frac{\alpha x_m}{\alpha-1}$ for $\alpha > 1$
VaR Definition	$\mathrm{VaR}_\alpha = F_{S(T)}^{-1}(\alpha)$
CVaR Definition	$\mathrm{CVaR}_\alpha = \mathbb{E}[S(T)|S(T) \geq \mathrm{VaR}_\alpha]$

Table 5: Summary of key Compound Poisson Process formulas.

References

- Cont, R., & Tankov, P. (2004). *Financial Modelling with Jump Processes.* Chapman & Hall/CRC.

- McNeil, A. J., Frey, R., & Embrechts, P. (2015). *Quantitative Risk Management: Concepts, Techniques and Tools.* Princeton University Press.

- Ross, S. M. (2014). *Introduction to Probability Models.* Academic Press.

- Madan, D. B., & Seneta, E. (1990). The variance gamma model for share market returns. *Journal of Business*, 63(4), 511–524.